

Estimation of Antiproton Flux and \bar{P}/P Ratios : Interpretation of the New High Energy Data-Sets by BESS, CAPRICE and PAMELA.

Goutam Sau^{1*}, P. Guptaroy^{2†}, A. Bhattacharya^{3‡} & S. Bhattacharyya^{4§}

¹ Beramara RamChandrapur High School,
South 24-Pgs, 743609 (WB), India.

² Department of Physics, Raghunathpur College,
Raghunathpur-723133, Purulia, India.

³ Department of Physics,
Jadavpur University, Kolkata- 700032, India.

⁴ Physics and Applied Mathematics Unit (PAMU),
Indian Statistical Institute, Kolkata - 700108, India.

Abstract

Very recent high-precision measurements on antiproton fluxes and the antiproton-to-proton ratios by the PAMELA Collaboration at relatively much higher energies are by now available. The results with regard to antiproton production phenomena though spring no special surprises, sharply in contrast with and contradiction to the case of positron production at the same energy-range, we consider that the totality of data on antiproton production from the past experiments to the very recent PAMELA outburst to be a challenging exercise for interpretation in terms of the secondary production mechanisms alone, the galactic propagation model etc against the background of the ‘dark-matter’-related controversy. In the present work we assume the validity of the simple leaky box model, choose a simple particle production model and attempt at providing a comprehensive interpretation of the totality of data on both antiproton flux measurements and the \bar{P}/P ratio-values for the various experiments ranging from BESS, CAPRICE and the PAMELA experiment at last. With the assumption of no contribution from the exotic sources to the antiproton production process, our model and the method describe the totality of the measured data with a fair degree of success.

Keywords: Cosmic rays high-energy interaction, Cosmic rays energy spectra, Cosmic rays galactic and extragalactic, Dark Matter

PACS nos.: 13.85.Tp, 96.50.Sb, 98.70.Sa, 95.35.+d

*e-mail:sau_goutam@yahoo.com

†e-mail:gpradeepa@rediffmail.com

‡e-mail:aparaajita_bh@yahoo.co.in

§e-mail: bsubrata@www.isical.ac.in (Communicating Author).

1 Introduction

In recent times the cosmic ray(CR) antiproton and positron flux measurements have assumed much heightened importance, as they could signal, it is believed by the theorists, to the indirect detection of dark matter. In fact, the tremendous surge of interest on the very recent PAMELA experiments centres around this pivotal expectation. Quite agreeably, the PAMELA experiments on antiproton production[1] is so far not very controversy-ridden. The centrestage of controversy really lies with the measurements and revelations of the positron excess measurements by the same PAMELA group[2]. And in a previous publication we dealt with[3] the same.

In the astroparticle sector the observed particles fall under two categories : primaries and secondaries. The primaries are considered to be those which are accelerated by astrophysical objects of our galaxy and comprise of electrons, protons, other light and heavier nuclei[4]. In the course of its journey in the space these energetic primaries undergo the process of spallation on the Interstellar Medium (ISM) mainly with the components Hydrogen and Helium. Besides, they also suffer energy losses by successive high energy interactions in the Earth's atmosphere while passing through the earth. After their production from the supernovae remnants, cosmic rays traverse and propagate in the galactic turbulent magnetic field, experience some deflections and finally enter the Earth. Both the spallation process and the interactions of the primaries with the ISM give rise to the various secondaries of which the antimatter particles, e.g., positrons, antiprotons etc. constitute a considerable part. For antiproton production spallation of secondaries too might play some role, though for all practical purposes we will certainly neglect such tertiary mode of production.

The concept of dark matter and its coupling to the Standard Model (SM) sector allows some annihilation or decay chains which could be additional sources of both matter and antimatter in equal measure. But in the general background matter is much more abundant than antimatter. So, it is understandable that the primary component due to so-called Dark Matter has better chance to be found[5] among antimatter cosmic rays.

In view of the importance of antiproton research in appreciating the role of production and propagation of primary cosmic rays, we have motivated ourselves here to find a compatibility of the various data-sets and to apply one single model for explaining the diverse observations made and reported by separate and several groups like, BESS'95[6], BESS'97[6], BESS'99[7], BESS'00[7], BESS'02[8] etc., CAPRICE'98[9] and PAMELA(2008)[1].

In the present work we will assort the data on antiproton flux measurements and the \bar{P}/P ratios by BESS[1995 - 2002], CAPRICE[1998] and PAMELA groups and try to understand the totality of data in a comprehensive manner with the clear emphasis laid on the latest PAMELA results.

2 Mechanism for Antiproton Production and the Expression for Invariant Cross Sections

According to the present version of the model the low- p_T (soft) baryon-antibaryons are produced through the decays of secondary pions of which proton-antiproton pairs comprise nearly one third. Bandyopadhyay and Bhattacharyya[10] and Bandyopadhyay et al[11] have worked out the details of the necessary field-theoretic calculations based on Feynman diagrams and obtained the following formulae for inclusive cross-sections at low- p_T valid for moderately high to high energies and by the average antiproton multiplicity

$$E \frac{d^3\sigma}{dp^3} |_{pp \rightarrow \bar{p}X} \simeq 1.87 * \exp[-7.38 \frac{p_T^2 + m_{\bar{p}}^2}{1 - x}] \exp[-5.08x] \quad (1)$$

and

$$\langle n_{\bar{p}} \rangle \simeq 1.08 * 10^{-2} S^{2/5} \quad \text{for } \sqrt{S} \leq 100 \text{ GeV} \quad (2)$$

$$\langle n_{\bar{p}} \rangle \simeq 2 * 10^{-2} S^{1/4} \quad \text{for } \sqrt{S} > 100 \text{ GeV} \quad (3)$$

where $m_{\bar{p}}$ is the mass of the antiproton and $n_{\bar{p}}$ is the measured antiproton multiplicity. With (2) we get at $\sqrt{S}=53 \text{ GeV}$, $\langle n_{\bar{p}} \rangle \simeq 0.2$ for both the formulae.

The crucial triumphs of this model are : i) It gives dynamically a unified picture of both low- and large-transverse-momentum phenomena and admits of no compartmentalization between soft and hard production of particles which is an artifact from the dictates of the Standard Model in particle physics. The only difference between them, according to this model, is in kinematics and in one additional feature of constituent rearrangement at high p_T . ii) It explains the $\ll \text{universality} \gg$ property of high-energy lepton-hadron, hadron-hadron, hadron-nucleus collisions and e^+e^- reactions in a nice dynamical and unambiguous way. iii) It subscribes to the ideas of jettiness of particle production at high energies in the form of two-sided $\ll \text{sprays} \gg$ of sequential arrays of hadrons. iv) It explains the by-now established leading-particle effect (LPE) in high- and very-high-energy collisions in a very satisfactory manner. v) Save and except a single parametrization, wherein there

is a degree of uncertainty, there is no hand-inserted parameter in the model. The model proposes a power law multiplicity for high-energy particle production and introduce Feynman scaling violation in an inbuilt manner even for relatively low-transverse-momentum region. For exceedingly low- p_T region a logarithmic nature of multiplicity might work and Feynman scaling might be valid under some stringent conditions and some strict restrictions. Naturally, this region is very limited and only a case for exception. vi) Last but not the least, another potential success of the model lies in its ability to explain the very slow rise of K/π ratio emphasized[12, 13] even very recently.

3 Estimation of Antiproton Flux and the \bar{P}/P Ratios

This Section is divided into the following few subsections and the undernoted subtitles.

3.1 Primary Spectra, Secondary Antiproton Production Model and the Working Formulae

In actual evaluation the model dependence comes into picture for getting values of $d\bar{\sigma}/dE$ which is related with the inclusive cross-section in the following way[14] :

$$\frac{d\bar{\sigma}}{dE} = \frac{\pi}{p_L} \int (E \frac{d^3\sigma}{dp^3})_{pp \rightarrow \bar{p}X} dp_T^2 \quad (4)$$

Here we take $p_L \simeq E$ as the transverse momenta of the produced secondary antiprotons is assumed to be small.

Inserting expressions (1), (2) and (3), our model-derived formula for inclusive cross-section valid at moderately high energies in eqn.(4) and integrating over p_T with normal approximations we get

$$\frac{d\bar{\sigma}}{dE}|_{p \rightarrow \bar{p}} \simeq 0.496 \exp[-5.08x] \quad (5)$$

where we have used the low-transverse-momentum upper limit up to $p_T = 1$ GeV/c. It must also be recalled that $p_L \simeq E$. Bhattacharyya and Pal[15, 16] have worked out that the antiproton-to-proton ratio is to be given finally by

$$f_{\bar{p}}(E) = \frac{J_{\bar{p}}(E)}{J_p(E)} = \frac{2K\lambda_e(E)}{m_p} \int_0^{X_s} E \frac{d\sigma_p}{dE} X^{\gamma-1} dx \quad (6)$$

where where J_p and $J_{\bar{p}}$ are the differential fluxes of the primary protons and the secondary antiprotons($m^{-2}sr^{-2}s^{-1}GeV^{-1}$) respectively. K is the correction coefficient taking into consideration the composition of the primary cosmic rays and the interstellar gas, $\lambda_e(E)$ is the average

path length of antiprotons against escape (gcm^{-2} as the unit), m_p is the mass of the proton (g as the unit), E_p is the total energy of the primary proton, E_s is the integral lower limit relevant to the production threshold of antiprotons, γ is the integral energy spectrum exponential of the primary protons and is the sole quantity taken from cosmic-ray information and it is used $\gamma=1.75$, $X = E/E_p$ and $X_s = E_s/E_p$ (we took $X_s \simeq -(m_p c^2/E) + [(m_p c^2/E)^2 + 1]^{1/2}$).

Usually, J_p is expressed as

$$J_p(E_p) = J_0 E_p^{-(\gamma+1)} \quad (7)$$

Now using eqn.(5), eqn.(7) in eqn.(6) we get

$$\frac{f_{\bar{P}}(E)}{K\lambda_e(E)} = \frac{2}{m_p} \int_0^{X_s} 0.496 \exp[-5.08x] x^{\gamma-1} dx \quad (8)$$

Here, we have always used $K = 1.26$, $\lambda_e = 5 \text{ gcm}^{-2}$ and $m_p \simeq 1 \text{ GeV}$.

3.2 The Effect of Annihilation Channels : A Damping Effect

At the relatively lower energy sides of ultra high energy interactions, both proton-antiprotons might enter into some annihilation reactions which would suppress the production ratio of \bar{P}/P in the main. In order to accommodate this probability we assume a damping correction term for the \bar{P}/P -ratios to be parameterized by $\sim \phi \exp[-\alpha E_{\bar{P}}^{\epsilon}]$ where ϕ , α and ϵ are the chosen parameters and $E_{\bar{P}}$ is the measured antiproton energy. We assume here that only the ratio-values of \bar{P}/P would suffer this diminutive change as the annihilations involve both the protons and antiprotons, though the individualized production of both protons and antiprotons would be considered to remain unaffected. The used values of ϕ , α and ϵ are 0.55, 0.7 and 0.5 respectively.

3.3 Choice of the Working Primary Proton Spectra

It is to be observed that the value of $f_{\bar{P}}(E)/K\lambda_e(E)$ is sensitive to the value γ and the value of γ could be different in different regions of the primary proton energy. But we have left out this issue for the present with the acceptance of a specific value of $\gamma = 1.75$ throughout this entire work. In order to proceed we have found the relationship between the secondary antiproton energy and the primary proton energy to follow the nature depicted by figure 1(a).

In figure 1(b), the median energy of primary protons is shown as a function of the secondary antiproton energy. It was found earlier that for antiproton energies of 3-9 GeV, which were relevant

to the experimental work performed until then, the median energies of primary protons were about 25-80 GeV. The present energy-region is somewhat higher. But we take the cue from Tan and Ng[14] and proceed in a similar manner to draw the figures shown in figure 1(b) and figure 1(c) as described in the figure-captions in some detail. Very carefully, we have chosen a modestly accurate primary proton spectrum. Modifying Badhwar et al[17] , we use here

$$J_P(E_P) = 2 * 10^5 E_P^{-2.75} \quad (9)$$

where $J_P(E_P)$ is in protons $m^{-2}sr^{-2}s^{-1}GeV^{-1}$.

Using this spectrum and our invariant cross section formulae, we have calculated the $f_{\bar{P}}(E)/K\lambda_e(E)$ curve as given in figure 1(c).

4 Results

The final results have here been actually worked out on the basis of the following two deduced expressions :

$$f'_{\bar{P}}(E_{\bar{P}}) = f_{\bar{P}}(E)J_P(E_P) \quad (10)$$

and

$$R_{\bar{P}}(E_{\bar{P}}) = \frac{J_{\bar{P}}(E)}{J_p(E)} * \phi \exp[-\alpha E_{\bar{P}}^{\epsilon}] = \frac{2K\lambda_e(E)}{m_p} \int_0^{X_s} E \frac{d\sigma_p}{dE} X^{\gamma-1} dx * \phi \exp[-\alpha E_{\bar{P}}^{\epsilon}] \quad (11)$$

The graphical plots drawn in figure 2 and figure 3 with expression (10) describe the nature of relatively low-energy antiproton-data measured by BESS, CAPRICE on antiproton flux. And the plot of model-based \bar{P}/P ratio-values based on expression (11) are displayed in figure 4 and figure 5 against the data-background. The used values of the parameters are shown in the adjoining table (Table 1).

5 Concluding Remarks

The entire data-sets measured by three distinctly separate groups at somewhat different energy-ranges of the proton primaries have been described here modestly satisfactorily. In our conclusions we have not taken into consideration any exotic source of antiprotons. So, no specific support to the concept of ‘dark matter’ could be rendered by our calculations and method; rather in a tacit manner the idea is disfavored. This is in contrast with the contentions of Buchmüller et al[18].

Table 1: Chosen values of the parameters

$\lambda_e(gcm^{-2})$	$m_p(GeV)$	γ	K	ϕ	α	ϵ
1.26	$\simeq 1.00$	1.75	5.00	0.55	0.70	0.50

We have based our calculations here on the Simple Leaky Box Model (SLBM). Even our previous work on positron results[3] by PAMELA group[2] was also done with the same propagation model, viz, SLBM. So the emphasis laid on the Nested Leaky Box Model by Cowsik and Burch[19, 20] on understanding the PAMELA-data related to the detection of positron excess is not substantiated by our works. Besides, the fair agreement between calculations and measurements provides a support to the secondary antiproton production model put into use here. In our approach there are a few chosen parameters which cannot be clearly accounted for right now from the physical considerations. This definitely constitutes some strong limitations to our success in interpretation of the data-trends.

References

- [1] O. Adriani et al : Phys. Rev. Lett. **102** (2009) 051101 [astro-ph/0810.4994 v2 25 February 2009].
- [2] O. Adriani et al : Nature **458** (2009) 607-609.
- [3] Goutam Sau, S.K.Biswas and S.Bhattacharyya : Hadronic Journal **31** (2008) 529.
- [4] T. Delahaye, P. Brun, F. Donato, N. Fornengo, J. Lavalle, R. Lineros, R. Taillet and P. Salati : hep-ph/0905.2144 v1 13 May 2009.
- [5] Arnon Dar : astro-ph.HE/0906.0973 v1 04 June 2009.
- [6] S. Orito et al : Phys. Rev. Lett. **84** (2000) 1078-1081 [astro-ph/9906426 v1 26 June 1999].
- [7] Y. Asaoka et al : Phys. Rev. Lett. **88** (2002) 051101 [astro-ph/0109007 v2 25 January 2002].
- [8] S. Haino et al : 29th International Cosmic Ray Conference, Pune **3** (2005) 13-16.
- [9] M. Boezio et al : The Astrophysical Journal **561** (2001) 787.
- [10] P. Bandyopadhyay and S. Bhattacharyya : Nuovo Cimento **A**, **43** (1978) 323.
- [11] P. Bandyopadhyay, R. K. Roy Chowdhury, S. Bhattacharyya and D. P. Bhattacharyya : Nuovo Cimento **A**, **50** (1979) 133.
- [12] T. T. Chou, C. N. Yang and E. Yen : Phys. Rev. Lett. **54** (1985) 510.
- [13] Bonn-Brussels-Cambridge-CERN-Stockholm-UA5 Collaboration (G. J. Alner et al) : Nucl. Phys. **B**, **258** (1985) 505.
- [14] L. C. Tan and L. K. Ng : J. Phys. **G**, **7** (1981) 123.
- [15] S. Bhattacharyya and P. Pal : IL Nuovo Cimento **C**, **9** (1986) 961.
- [16] S. Bhattacharyya and D. Roy : Mod. Phys. Letts. **A**, **13** (1998) 2173.
- [17] G. D. Badhwar, S. A. Stephens and R. L. Golden : Phys. Rev. **D**, **15** (1977) 820.
- [18] W. Buchmüller, A. Ibarra, T. Shindou, F. Takayama and D. Tran : hep-ph/0906.1187 v1 5 June 2009.
- [19] R. Cowsik and B. Burch : astro-ph.CO/0905.2136 v2 11 June 2009.
- [20] R. Cowsik and B. Burch : astro-ph.CO/0906.2365 v1 12 June 2009.

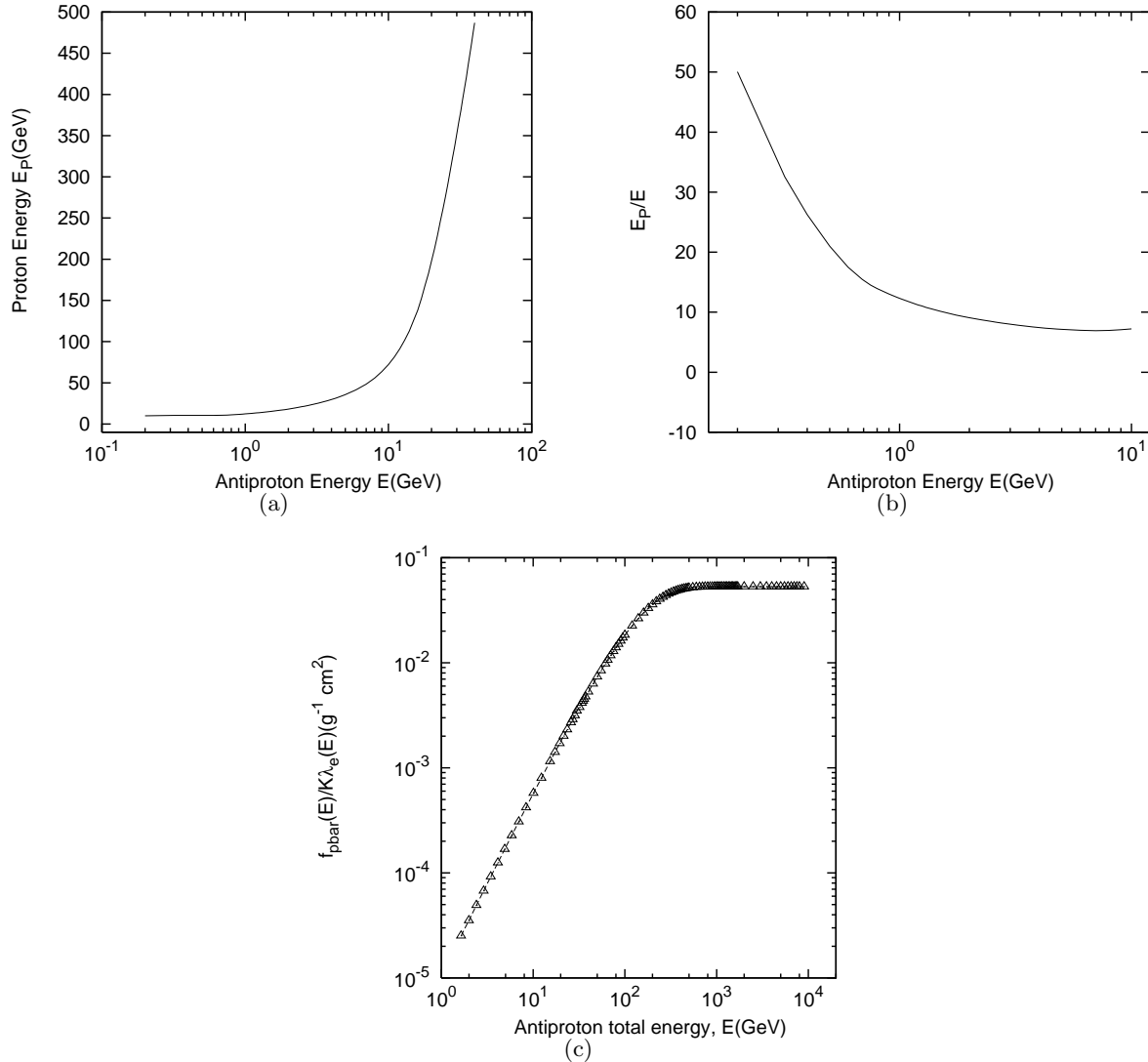


Figure 1: (a) Plot of the relationship between the variation of antiproton energy (E) and primary proton energy (E_P), (b) Relation between primary proton energy (E_P) and the total antiproton energies (E); the plot has been done on E_P/E (Y-axis) against E (X-axis), (c) The calculated antiproton to proton flux ratio (in terms of $K/\lambda_e(E)$) against the antiproton energy E .

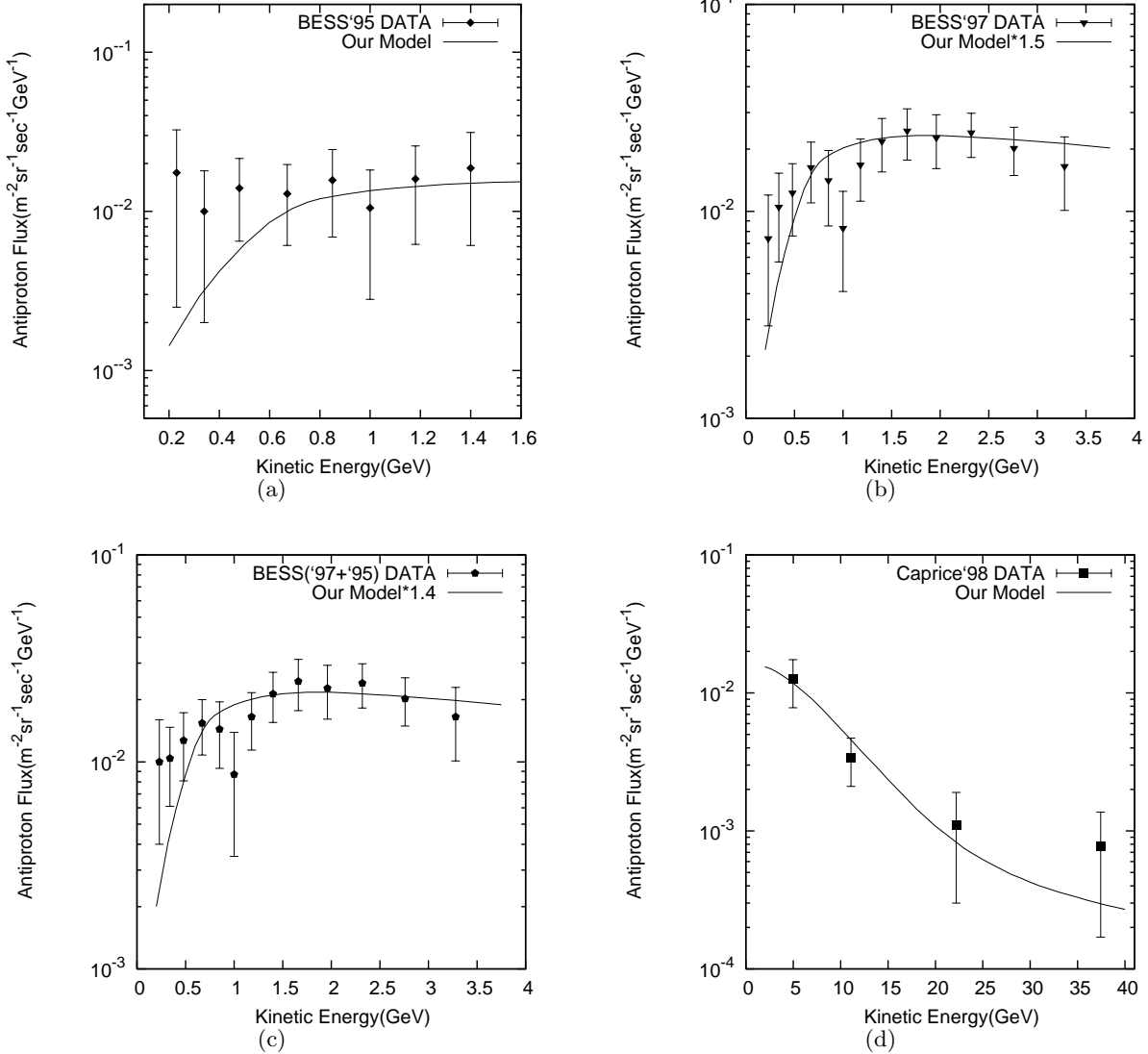


Figure 2: Antiproton fluxes at the top of the atmosphere as measured by BESS'95[2(a)], BESS'97[2(b)], BESS('97+'95)[2(c)] and Caprice'98[2(d)]. The solid lines represent the calculations based on our theoretical model (10). The experimental data are collected from Ref.[6, 9]

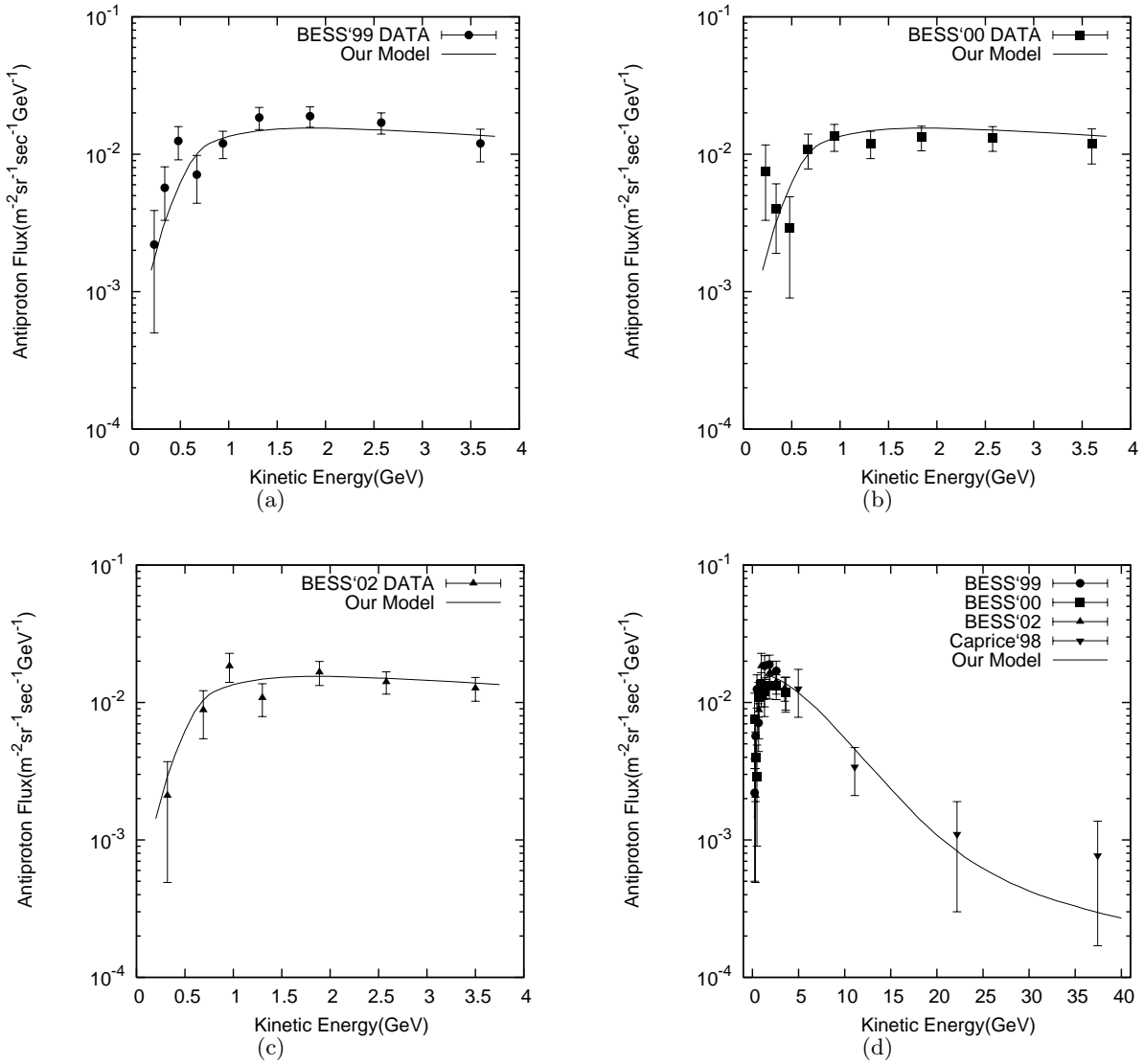


Figure 3: BESS'99[3(a)], BESS'00[3(b)], BESS'02[3(b)] and together of BESS, CAPRICE[3(c)] Antiproton fluxes at the top of the atmosphere. The solid curves shows the calculations of our theoretical model (10). The experimental data are collected from Ref.[7, 8, 9]

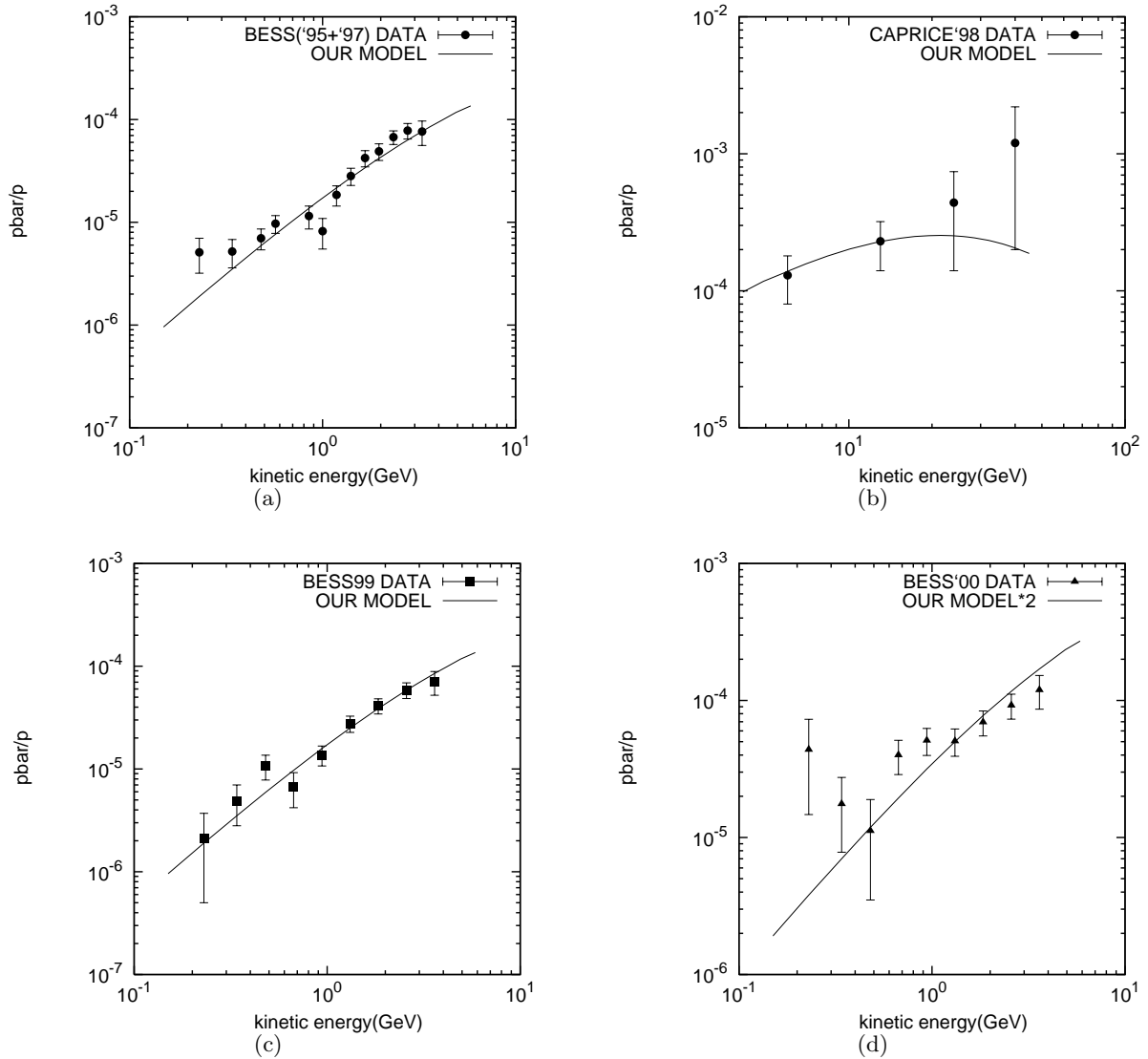


Figure 4: Plot of \bar{P}/P ratios measured by BESS ('95+'97)[4(a)], CAPRICE'98[4(b)], BESS'99[4(c)] and BESS'00[4(d)]. The solid curves represent our calculations based on our model based approach (11). The experimental data are collected from Ref.[6, 9, 7]

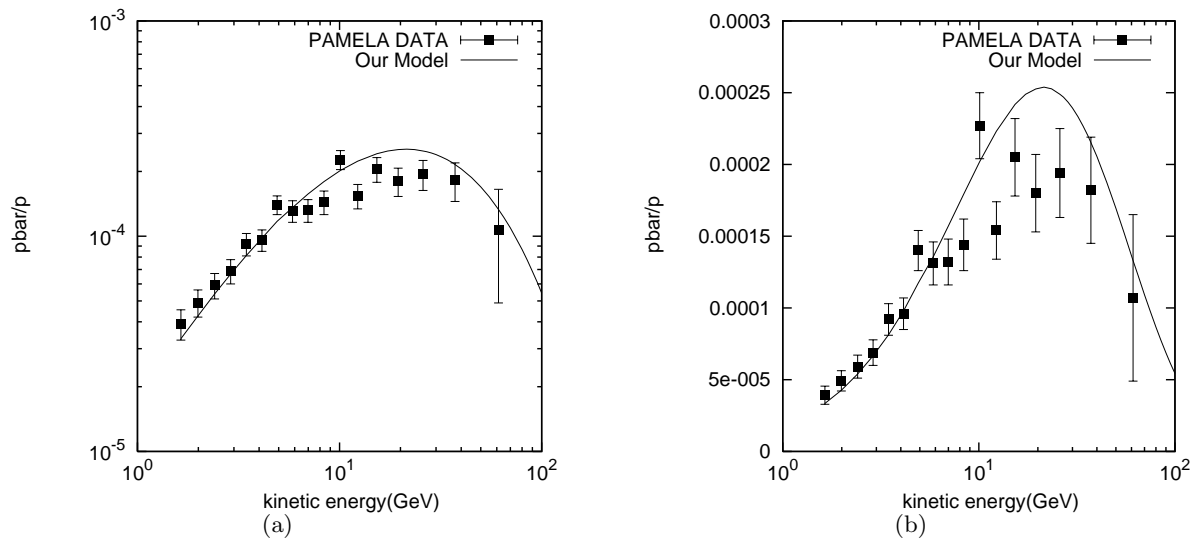


Figure 5: Plot of \bar{P}/P ratios measured by PAMELA group and the solid curves represent our calculations based on our model based approach (11). The experimental data are collected from Ref.[1]